

Total water vapor column retrieval from MSG-SEVIRI split window measurements exploiting the daily cycle of land surface temperatures

M. Schroedter-Homscheidt^{a,*}, A. Drews^{b,1}, S. Heise^c

^a Deutsches Zentrum für Luft- und Raumfahrt (DLR) e.V., Deutsches Fernerkundungsdatenzentrum (DFD), Oberpfaffenhofen, 82234 Wessling, Germany

^b Carl von Ossietzky Universität Oldenburg, Institut für Physik, Germany; former affiliation Georg-August-Universität Göttingen / Deutsches Zentrum für Luft- und Raumfahrt (DLR) e.V., Germany

^c GeoForschungsZentrum Potsdam, Department of Geodesy and Remote Sensing, Germany

Received 24 November 2005; received in revised form 3 May 2007; accepted 5 May 2007

Abstract

A physically based algorithm for the retrieval of total water vapor column (TWC) over cloud-free land surfaces proposed by Kleespies and McMillin [Kleespies, J.T., McMillin L.M. (1990). Retrieval of precipitable water from observations in the Split Window over varying surface temperatures. *Journal of Applied Meteorology*, 29, 851–862.] is evaluated and extended for use in atmospheric correction and surface irradiance calculation schemes. Thermal infrared split window channels at 10.8 and 12.0 μm of the MSG-SEVIRI (Meteosat Second Generation-Spinning Enhanced Visible and Infrared Imager) instrument are used. The proposed algorithm takes advantage of the improved measurement capabilities of the MSG-SEVIRI instrument with its 15 min temporal resolution and its radiometric accuracy of 0.25 K and 0.37 K in the 10.8 and 12.0 μm channels. The temporal resolution allows exploitation of the daily land surface temperature variation. There is no further need for explicit auxiliary information on air and land surface temperatures, which is difficult to obtain on an operational basis. Updated coefficients for the split window parameterization are derived based on simulations of ‘top-of-atmosphere’ SEVIRI brightness temperatures for the globally representative Thermodynamic Initial Guess Retrieval (TIGR3) set of radiosonde profiles. It turns out that the linear dependency on the transmission ratio in both split window channels as originally proposed by Kleespies & McMillin [Kleespies, J.T., McMillin L.M. (1990). Retrieval of precipitable water from observations in the Split Window over varying surface temperatures. *Journal of Applied Meteorology*, 29, 851–862.] has to be extended towards a non-linear approach in order to make it applicable to the full range of global atmospheric conditions. Sensitivity studies reveal that the parameterization relies on the availability of input brightness temperatures with a variation larger than approximately 5 K during the daily cycle. The new TWC algorithm was tested with MSG-SEVIRI data for European and African regions for the period March–August 2004 and compared with radiosonde data. The results show that the algorithm is capable of producing TWC values with a mean bias of -0.2 mm and an RMSE of 6.8 mm. From the total amount of 2583 coincidences for all viewing zenith angles both for winter and summer conditions, 82% were within a ± 5 mm and 94% were within a ± 10 mm difference interval between MSG-based and radiosonde-based TWC. A second comparison to European GPS measurements for the same period from March to August 2004 reveals a bias of -3.0 mm and an RMSE of 6.0 mm. This result is obtained for 11 UTC GPS measurements which proved to match best the MSG-TWC values. Comparing MSG-TWC to daily cloud-free mean GPS values shows a lower bias of -2.56 mm and an increased RMSE of 6.6 mm. These findings support the usefulness of the new MSG-based algorithm for surface irradiance calculations and atmospheric correction purposes.

© 2007 Elsevier Inc. All rights reserved.

Keywords: Total water vapor column; Split window; Infrared; MSG; SEVIRI; Daily land surface temperature cycle

* Corresponding author. Tel.: +49 8153 28 28 96, fax: +49 8153 28 13 63.

E-mail address: marion.schroedter-homscheidt@dlr.de

(M. Schroedter-Homscheidt).

¹ Both M. Schroedter-Homscheidt and A. Drews are members of the Helmholtz Association virtual Institute of Energy Meteorology (vIEM).

1. Introduction

Total water vapor column (TWC) is one of the most important absorbers in the atmosphere, showing a non-linear interaction

with the radiation field. Therefore, TWC measurements are needed for atmospheric correction of satellite based surface measurements and as additional information to retrieve other geophysical parameters, such as e.g., surface irradiation, aerosols, land surface temperature, land use parameters, or the normalized differential vegetation index. Holzer-Popp et al. (2001) show that TWC for instantaneous values should be known better than 10 mm for an atmospheric correction of surface albedo better than 0.01. Therefore, this study aims at a retrieval method with a low bias and RMSE of better than 10 mm which can be used for large data sets in near real time without the need for external auxiliary information available, e.g., only at national weather services.

Besides atmospheric correction the driving application for this work is the use of solar surface irradiance information for energy and architecture applications. Information on solar surface irradiance is a prerequisite for renewable energy technologies like photovoltaic and concentrating solar thermal power plants. Successful integration of solar energy in existing energy supply structures depends on exact knowledge about the highly variable solar resource. Conventional energy production is also affected as surface irradiance is the second most relevant input parameter after air temperature for electricity load forecasting. Müller (2001) state the need for accuracy better than 15% for TWC information in daily resolution for solar energy applications. Besides the energy business, solar surface irradiance measurements are also used as information on available daylight in architecture and urban planning.

The Meteosat Second Generation (MSG) satellite series with its Spinning Enhanced Visible and Infrared Imager (SEVIRI) offers new possibilities as it measures ‘top-of-atmosphere’ radiances and reflectances with a temporal resolution of 15 min and a spatial resolution of 3 km at the sub-satellite point in 11 spectral channels at 0.6, 0.8, 1.6, 3.9, 6.2, 7.3, 8.7, 9.6, 10.8, 12.0, and 13.4 μm . The excellent temporal resolution especially allows exploitation of the daily cycle of measurements, while the spatial resolution is important for cloud detection with a horizontal resolution of few kilometers. In comparison with the ATOVS (Advanced TIROS Operational Vertical Sounder) instrument suite on board the NOAA (National Oceanic & Atmospheric Administration) satellite series, which was used up to now for atmospheric correction purposes, this improves the horizontal resolution by a factor of more than 10 in cloud-free regions over Europe and Africa.

Measurements in the 10.8 and 12.0 μm channels have been widely used to retrieve total water vapor content. The differential water vapor absorption in both channels allows estimation of water vapor column between the surface and top of the atmosphere. Split window channels are affected by the surface, the mean air temperature, and additionally by atmospheric absorption, which is mainly caused by water vapor in this spectral region. In principle both surface and mean air temperature are necessary additional information for deriving water vapor column from a single channel measurement. Using measurements in the two split window channels, either surface or mean air temperature dependence can be eliminated, but one of them still has to be known. Chesters et al.

(1983, 1987) apply such an approach to the VISSR Atmospheric Sounder (VAS) on board the Geostationary Operational Environmental Satellites (GOES). They use radiosonde information as auxiliary information to estimate the mean air temperature. This requirement is a serious drawback for stand-alone processing outside a weather service processing system as air temperature data is difficult to access operationally in near real time.

The EUMETSAT Nowcasting-SAF proposes deriving mean air temperature from the 13.4 μm channel (EUMETSAT NWC-SAF, 2005). As this channel is sensitive for the lower atmosphere and less sensitive for the surface signal, it allows a rough estimate of mean air temperature of the lower atmosphere.

As an alternative approach, the Physical Split Window technique (PSW, Guillory & Jedlovec, 1993; Jedlovec, 1987; Suggs et al., 1998) is used for the operational GOES total precipitable water vapor product provided by NOAA. The PSW approach uses a perturbation formulation of a simplified radiative transfer equation to derive boundary layer water vapor information. It also requires a priori information as first guess taken from a numerical prediction model or radiosonde measurements.

Besides these approaches to derive additional air temperature information, Kleespies and McMillin (1984, 1990) propose using the split window channels under conditions of changing surface temperatures to overcome these restrictions. The use of measurements in two situations with changing surface temperatures allows an extended equation system to be set up and eliminates both surface and air temperature as input parameters. On the other hand it relies on the assumption of an unchanged atmosphere between these two situations. Kleespies and McMillan tested their algorithm both on the VAS instrument using changes in surface temperature during the daily temperature cycle and on the NOAA Advanced Very High Resolution Radiometer (AVHRR) using changes in surface temperature between land and ocean surfaces. Both methods could be applied only in a restricted number of test cases. It turned out that the VAS radiometric accuracy was not sufficient and therefore measurement noise inhibited the successful use of that instrument. For the few AVHRR cases used, the method worked well but was restricted to single cases with a strong temperature gradient between land and sea in coastal regions. The new MSG-SEVIRI instrument characteristics help to overcome both restrictions, as the daily cycle of surface temperature can be monitored and the radiometric accuracy is sufficient with 0.25 K and 0.37 K at 300 K (Schmetz et al., 2002). Therefore, this paper evaluates the use of the method proposed by Kleespies and McMillan for MSG-SEVIRI measurements over European and African land surfaces.

Section 2 introduces the Kleespies and McMillan method and the test data set chosen to evaluate this method. Section 3 shows results of this evaluation. These simulations motivate an extension of the Kleespies and McMillan method which is presented together with sensitivity analyses and sample results. Validation comparing the new method to European and African radiosondes and GPS measurements is given in Section 4, while Section 5 discusses the results obtained.

2. Theory and test data set

2.1. Theory of Kleespies & McMillan method

Split window algorithms exploit the difference in water vapor absorption between the 10.8 and the 12 μm channels. The ratio of atmospheric transmittances in the two channels is related to total water vapor column. In general, infrared ‘top-of-atmosphere’ brightness temperature measured at the satellite is affected by surface temperature T_S , mean air temperature T_A , surface emissivity ϵ , water vapor, and absorption of other atmospheric gases. ‘Split window’ channels are selected close to each other, so that equal emissivity and absorption of gases other than water vapor can be assumed. Surface temperature is the same for both channels and can be eliminated. Following [Chesters et al. \(1983\)](#) and [Kleespies and McMillin \(1984\)](#) TWC can be related to brightness temperature measurements $T_{B,11}$ and $T_{B,12}$ at 10.8 and 12 μm as follows

$$TWC = fct \left[\frac{1}{\sec\theta} \ln \left(\frac{T_{B,11} - T_A}{T_{B,12} - T_A} \right) \right] \quad (1)$$

For this relationship local linearity of the Planck function is assumed together with a single thick layer containing the total water vapor. In order to derive total water vapor content, air temperature still has to be known. To avoid this dependence, two situations with varying surface temperatures are selected. Having these two equations the air temperature dependence can be eliminated (for a full mathematical derivation see [Kleespies & McMillin, 1990](#)) if it is assumed that the atmospheric state is approximately the same in both situations. This allows us to describe TWC as a function of brightness temperatures and satellite zenith angle θ

$$TWC = fct \left[\frac{1}{\sec\theta} \ln \left(\frac{T_{B,11}^a - T_{B,11}^b}{T_{B,12}^a - T_{B,12}^b} \right) \right] \quad (2)$$

with a and b indicating brightness temperature measurements in two different situations. MSG can provide these two situations with varying surface temperatures but a constant viewing geometry during the daily temperature cycle over land.

2.2. Test data set

The Thermodynamic Initial Guess Retrieval (TIGR3, [Chédin et al., 1985](#)) data set was developed at the Laboratoire de Météorologie Dynamique (LMD, Paris) especially for retrieval development. It includes more than 2300 radiosonde profiles from all over the world. The profiles are selected to represent the maximum variability of atmospheric temperature and humidity conditions. This means that besides standard atmospheric profiles, extreme situations are also collected covering the full atmospheric range from the tropics to the polar regions. Temperature, humidity, and ozone are given for each profile at 40 vertical levels between 1013 and 0.05 hPa together with latitude and longitude of the radiosonde station.

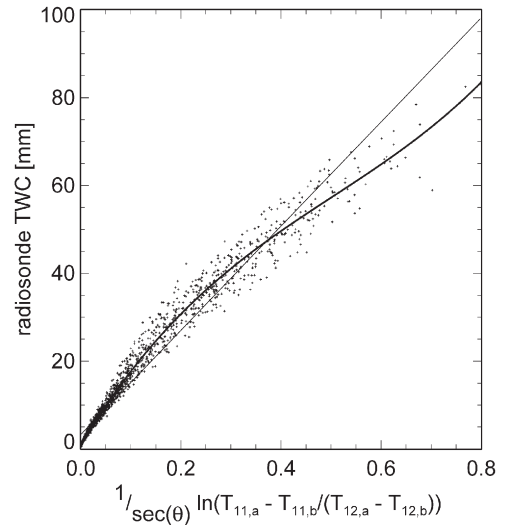


Fig. 1. TWC as given in the TIGR3 radiosonde data set vs. transmission ratio term as defined in Eq. (1). [Kleespies and McMillin \(1990\)](#) proposed a linear relationship (thin line) while the analysis of a larger data set of 2300 radiosondes reveals non-linear behavior e.g. described with a third order polynomial (thick line).

All TIGR3 profiles were integrated vertically to calculate ‘true’ TWC. Forward radiative transfer calculations using MODTRAN 3.7 ([Abreu & Anderson, 1996](#); [Berk et al., 1999](#)) were performed to simulate MSG satellite measurements in the 10.8 and 12 μm channels.

3. Method and evaluation

3.1. The proposed method

[Kleespies and McMillin \(1990\)](#) assessed the functional relationship between transmission ratio and TWC empirically through comparisons with North American radiosondes collected on three consecutive synoptic times on 8 June 1982. They proposed a linear dependence, but it should be noted that they already observed and discussed deviations from this linearity. This motivated the presented study with a larger radiosonde data set.

The Kleespies and McMillan algorithm was applied to simulated MSG brightness temperatures in order to derive TWC. [Fig. 1](#) shows the relationship between ‘true’ TWC values calculated from the TIGR3 radiosondes and the transmission ratio term introduced in Eq. (2). Testing the whole TIGR3 data set and several fit functions, it turned out that a third order polynomial (thick line) describes the relationship better than a linear fit (thin line) does as proposed by [Kleespies and McMillin \(1990\)](#).

$$TWC = a + b(\text{ratio}) + c(\text{ratio})^2 + d(\text{ratio})^3$$

$$\text{with ratio} = \frac{1}{\sec\theta} \ln \left(\frac{T_{B,11}^a - T_{B,11}^b}{T_{B,12}^a - T_{B,12}^b} \right) \quad (3)$$

Assumably, the reasons for this non-linear behavior are (a) non-neglectable absorption of other atmospheric gases such as

ozone, carbon dioxide, and methane if TWC is very small and (b) saturation of absorption lines for large TWC values.

Using this new approach, TWC derived from simulated MSG measurements was again compared with the ‘true’ TWC calculated directly from radiosondes. The comparison as shown in Fig. 2 revealed good agreement, with bias and RMSE of 1.2 and 1.6 mm, respectively. For these forward calculations the difference in surface temperature was assumed to be 5 K, the surface emissivity was set to a global average of 0.975, and coefficient values of 1.1, 187.7, -225.6 , and 149.8 for a, b, c, and d, respectively, were used. Table 1 gives an overview on these parameter settings (case ‘base’) together with the parameter variations used to derive the following results.

This approach assumed equal surface emissivity both in the 10.8 and the 12.0 μm channels, which is not true for all surfaces. A case study (‘sensitivity to ε ’, Table 1) was performed using the same polynomial fit function for the retrieval step as used above, but setting a surface emissivity of 0.97 for the 10.8 μm channel and of 0.985 for the 12.0 μm channel in the forward calculation of the simulated satellite signal. These surface emissivity values are representative for sand surfaces (Schmugge et al., 2002) and can be counted as an extreme deviation from the assumption of a constant surface emissivity of 0.975. This study resulted in a bias of 2.7 mm and an RMSE of 2.6 mm. This degradation is still acceptable for the application intended, especially taking into account that it is an extreme case study.

In an additional forward calculation run (‘SZA dependence’, Table 1), the fit function describing the relationship between TWC and the transmission ratio term was separately derived for different satellite zenith angles of 0, 20, 36.6, 40, 56.5 and 68.6°. The values of 36.6, 56.5 and 68.6° were chosen as they are valid for ground truth stations offering direct and spectral irradiance measurements. These stations were used in the European Heliosat-3 project on method development for surface irradiance calculations from Meteosat Second Generation satellite data and also in this study for

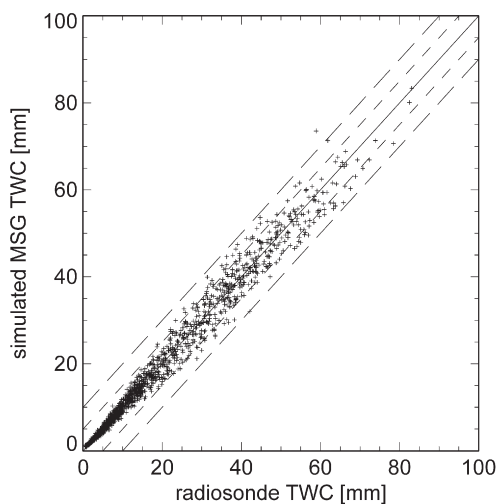


Fig. 2. TWC derived from simulated MSG-SEVIRI measurements using the proposed method vs. total water vapor column as given in the TIGR3 radiosonde database. Additional dashed lines indicate that the differences are well within an interval of ± 5 and ± 10 mm, while bias and RMSE are 1.2 and 1.6 mm, respectively.

Table 1
Parameter settings for radiative transfer simulations

Simulation study	ΔT_s [K]	$\varepsilon_{10.8}$	ε_{12}	Radiometric noise [K]	θ [°]
‘Base’	5	0.975	0.975	None	0
‘Sensitivity to ε ’	5	0.97	0.985	None	0
‘SZA dependence’	5	0.975	0.975	None	0, 20, 36.6, 40, 56.5, 68.6
‘Instrument noise’	5	0.975	0.975	0.25 for 10.8 μm 0.37 for 12.0 μm	0
‘Minimum ΔT_s ’	10	0.975	0.975	0.25 for 10.8 μm 0.37 for 12.0 μm	0

consistency reasons. A significant dependence on zenith angle was found. This is not surprising, as it is known that a cosine of the satellite zenith angle is only a first order approximation of the air mass effect. Nevertheless, an exact air mass correction for infrared channels requires knowledge of the air temperature profile, which in many cases will not be available for future operational use of the algorithm. Therefore, the dependence of the third order polynomial fit function coefficients on satellite zenith angle was evaluated to derive an empirical fit. This step can be omitted if a temperature profile is available, e.g., from numerical weather models or campaign data. Fig. 3 shows the fit function coefficients a, b, c, and d as a function of satellite zenith angle. Each curve was smooth enough to be fitted with a second order polynomial. The coefficients were calculated from

$$a = 0.0001\theta^2 - 0.0045\theta + 1.1092$$

$$b = 0.0094\theta^2 - 0.0685\theta + 188.0$$

$$c = -0.03\theta^2 + 0.1858\theta - 226.6$$

$$d = 0.0294\theta^2 - 0.1854\theta + 151.0 \quad (4)$$

It can be noticed that the coefficients of the third order polynomial (Eq. (3)) vary between large negative and positive values. In general, this is a signal that a polynomial is not an optimum fit function and may cause large fit errors outside the fitted value range or between data points used. Nevertheless, this is not relevant in this case as the underlying TIGR3 TWC data range between 0 and 80 mm fits the natural variability very well. Also, there are no gaps between data points (Fig. 1) which is an advantage of using the large TIGR3 data set covering the atmospheric variability for such a retrieval development.

3.2. Sensitivity analysis

Up to now an ideal satellite without any measurement noise was assumed. MSG is specified to have a radiometric noise of 0.25 K in the 10.8 μm channel and 0.37 in the 12 μm channel. As the transmission ratio term contains the difference of brightness temperatures, radiometric noise affects the accuracy of the method in cases of low difference of brightness temperatures. In order to assess a minimum value required for surface temperature difference in the two situations, two forward calculation runs

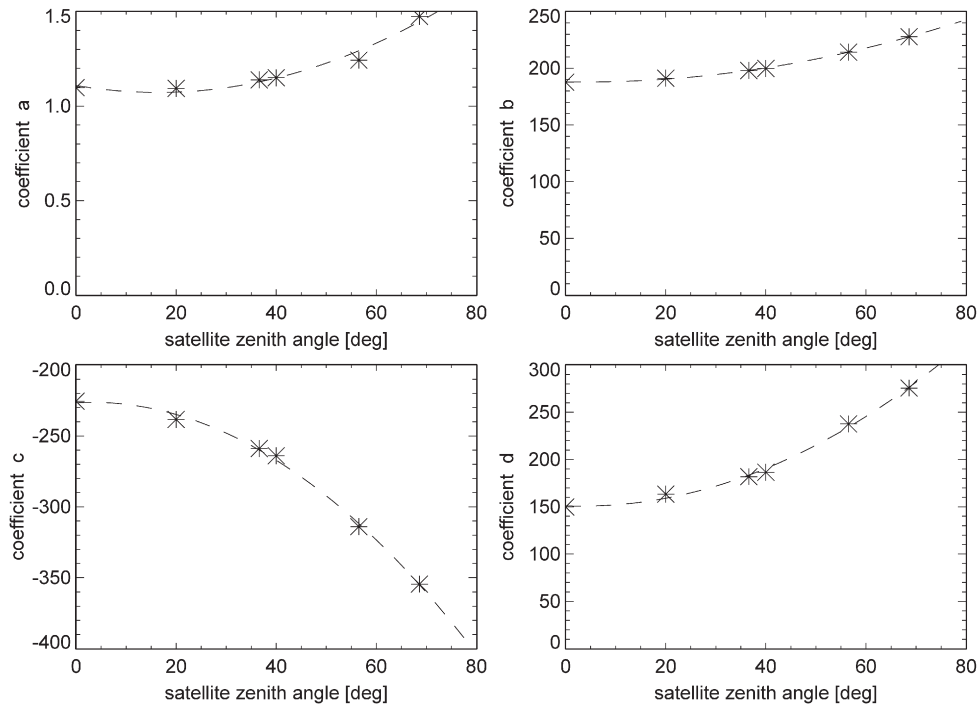


Fig. 3. Third order polynomial coefficients a, b, c, and d as functions of satellite zenith angle. Stars indicate simulations made for satellite zenith values of 0, 20, 36.6, 40, 56.5, and 68.6°. A significant dependence is found for each coefficient which can be approximated by a second order polynomial (dashed line).

using noisy signals with a random error of the size of the specified radiometric error and a 5 K difference ('instrument noise', Table 1) and 10 K difference in surface temperature were performed ('minimum ΔT_S ', Table 1). It turned out that the 5 K difference in surface temperature resulted in a bias and RMSE of 6.9 and 7.0 mm for a comparison between 'true' and retrieved values in this study. A 10 K difference in surface temperatures resulted in less scatter with bias and RMSE of 4.6 and 3.7 mm, respectively.

Such large positive biases due to the introduction of symmetric radiometric noise can be explained, as negative TWC values due to noisy data are excluded as impossible in the statistical analysis. Therefore, especially in the small TWC range only overestimation is counted in the statistics and due to the low signal-to-noise ratio in the small TWC range this overestimation is rather large.

As surface temperature is not known during the operational use of the algorithm, a minimum of 5 K difference in brightness temperatures in the 12 μm channel was requested in the current version. Choosing this minimum difference is a critical point for the algorithm as a low value increases the retrieval noise, while choosing a high value reduces the number of retrievals available. The currently used value of 5 K was also motivated by a study of Meßinger (1993) showing atmospheric correction of land surface temperatures as a function of 'top-of-atmosphere' brightness temperature and surface height both for winter and summer mid-latitude standard atmospheres. A typical difference in atmospheric correction between low and high brightness temperatures is in the range of 1–4 K. This has to be added to the requested brightness temperature difference of 5 K to determine surface temperature differences. Therefore, it was assumed that 5 K in brightness temperature difference results in a surface temperature difference well between 5 and 10 K motivated by the sensitivity

analysis. Nevertheless, even having these study results available, the setting of a minimum difference of 5 K was still not strictly defined. Finally, only a validation with several years of MSG data will help to find an optimum value. A first estimate using six months of MSG data is given in the validation section.

Setting this minimum difference value also raised the question of the availability of such data pairs over humid areas, snow or generally in winter. Land surface temperature measurements from the NOAA Advanced Very High Resolution Radiometer (AVHRR) available for March to October 1996 indicate that such an increase in surface temperature during the daily cycle is frequently available in cloud-free regions during spring, summer, and autumn months, also in northern Europe. Nevertheless, this question can also be answered only by validating large amounts of MSG data in different seasons, which is out of the scope of this paper.

3.3. Input data selection

Up to now results based on simulations were shown. For practical application of the proposed method, measurements of 'two situations with varying surface temperature' had to be found automatically. First, a cloud detection scheme excluded cloudy pixels in each 15 min SEVIRI image. The AVHRR Processing scheme Over cLOUDs, Land and Ocean (APOLLO, Gesell, 1989; Kriebel et al., 1989, 2003; Saunders & Kriebel, 1988) was adapted to MSG-SEVIRI for this purpose.

After cloud detection for each MSG pixel, a pair of cloud-free measurements between early morning and noon was selected. On the one hand measurements close to each other in time were looked for to fulfill the assumption of a constant atmosphere; on

the other hand a difference in brightness temperatures of more than 5 K was asked for in the current implementation.

The selection process starts after sunrise and looks for the first cloud-free measurement available for a pixel. Once this first measurement is found, a second measurement is looked for with a minimum time difference in between of 4 h. In case the measurement after this period is cloudy, the next 12 SEVIRI images are checked for a cloud-free case. As soon as two cloud-free measurements are found, the selection procedure is successful. So, the maximum time difference allowed is 7 h.

This selection procedure is a compromise. Certainly, the validity of assuming a constant TWC during this interval is a function of the atmospheric state and probably the major source of error. Taking into account a typical TWC correlation length of about 600 km (Lindau, 2004), the assumption of constant TWC over several hours is justified in many cases. Situations with fast moving air masses, strong TWC gradients, or intensive latent heat flux will limit the method. On the other hand, fast moving air masses are typically combined with heavy cloud cover and the algorithm is not applicable anyway. Anyhow, situations with intensive latent heat flux are typically situations where the required minimum difference in surface temperature is reached after a short time difference, which reduces the error.

An additional quality control of the input data was done implicitly as only transmission ratios between 0 and 0.8 were accepted in the retrieval. This was to avoid any non-detected unreliable values in the satellite signal, which were observed a few times causing extremely high and unrealistic transmission ratios. It is assumed that these values can be attributed to failures in the data reception. This choice corresponds to an allowed range of TWC from 0 to 80 mm, which is the maximum interval observed in the atmosphere for extreme arctic and tropical cases.

3.4. Sample results

Besides atmospheric correction and energy research applications which need products containing retrieved TWC values on a daily basis, this retrieval allows the generation of a TWC climatology based on cloud-free measurements for the MSG field of view. Obviously, several years of MSG-SEVIRI data are needed when setting up a climatology to get meaningful values in areas with frequent cloud cover. Nevertheless, a first impression of monthly mean TWC is given together with the one sigma variability and the number of retrievals available for the monthly mean generation for May and August 2004 (Fig. 4). These months were chosen as test cases for the HELIOSAT-3 project. White areas indicate values missing either due to cloud cover, the MSG field of view, or the presence of sea surface.

In the region of the intertropical convergence zone (ITCZ) a remarkable scatter was noticed which corresponds to a low number of retrievals available due to cloud cover during the averaging period. It is also assumed that the average especially in this region is affected by a negative bias, as the measurements are taken in cloud-free situations only, which means they represent dry situations more frequently.

4. Validation

4.1. Validation data set

TWC retrievals were compared to radiosonde measurements taken at 257 European and African stations provided by the British Atmospheric Data Center (BADC, <http://badc.nerc.ac.uk>). The data comprise vertical profiles of temperature and dew-point temperature at standard and significant pressure levels beginning in 1997. Stations conduct ascents up to four times daily at the synoptic hours of 00, 06, 12, and 18 UTC. TWC was calculated as a vertical integral from profiles of temperature and dew-point temperature.

MSG based TWC values were derived for Europe for the period from March to August 2004 and for the full field of view of MSG for May, July and August 2004. 2583 coincidences were found from MSG and 12 UTC radiosonde measurements. For these coincidences all MSG values within a 0.2° interval around the radiosonde station were averaged and compared to the radiosonde result. This interval was chosen to account for a typical drift of the radiosonde during its ascent and for the MSG-SEVIRI pixel size.

A second validation was performed using European GPS measurements taken at 295 stations and provided by the GeoforschungsZentrum Potsdam. Two-hourly available zenith path delays from 1 UTC to 23 UTC were transformed to TWC by using a scheme as described in Bevis et al. (1994). This data set was compared with the same MSG based TWC values from the period from March to August 2004 as used for the radiosonde comparison.

4.2. Validation results and discussion

Fig. 5 gives the histogram of differences of MSG-SEVIRI TWC minus radiosonde TWC measurements. The distribution showed a clear peak close to the zero difference, representing a mean bias error of -0.2 mm and an RMSE of 6.8 mm. Deviations from the zero difference were distributed nearly equally both for negative and positive differences.

Fig. 6 shows a two dimensional histogram for MSG-SEVIRI TWC versus radiosonde TWC measurements. A noteworthy scatter were noticed which results in a low correlation coefficient of 0.59. Nevertheless, a maximum of coincidences could be clearly identified around the identity line. Having the required accuracy of less than 10 mm in mind, it was noted that 94% of the differences were within a 10 mm range, and even 82% were within an even stricter 5 mm range. Therefore, the specified accuracy requirement is fulfilled. We assume that part of the scatter can be attributed to the comparison of a retrieval based on a pixel pair with several hours in between with the 12 UTC radiosonde measurement. As soon as the temporal variability is high this will cause significant scatter.

Another validation study was performed for a minimum required difference of 8 K instead of 5 K in input brightness temperatures in the $12 \mu\text{m}$ channel. This study revealed a mean bias error of -0.3 mm, a slightly decreased RMSE of 6.1 mm, and a correlation coefficient of 0.64. In this study 84% of coincidences were within a 5 mm range and 96% were within a 10 mm range.

These results were only slightly improved in comparison to a choice of 5 K as minimum difference in 12 μm brightness temperatures. Therefore, the required minimum difference of 5 K in the current implementation seemed acceptable, having also in mind that it improved the number of retrievals remarkably.

It should be noted that five of ten outliers with high values of the radiosondes above 30 mm and low values of the MSG TWC below 15 mm (Fig. 6) were measurements from the Jeddah radiosonde. This is a station where typically low water vapor content is expected. Comparing mean bias deviation and RMSE for each station, the Jeddah station was also suspected to have an extreme mean bias of -14.6 mm and an overall maximum RMSE value of 11.9 mm.

Attempts to identify a reason for the low correlation coefficient included a check of statistics of the observed differences against all input parameters, a check for any latitudinal dependence, and a test for a possible dependence of the differences on boundary layer air temperature values or profile structure using the available radiosonde information. Nevertheless, no significant results were observed in these studies.

We assumed that most of the scatter is due to miss-time and miss-distance effects between the drifting point measurement by the radiosonde and the MSG measurement which is averaging spatially inside a pixel and temporally during the morning hours. This motivated a semi-variogram analysis of the reference data set consisting of 257 radiosonde stations. Such an analysis allows a rough estimation of the effect of miss-time and miss-distance and an estimation of the accuracy which could be achieved if different radiosondes were replaced towards a single location. Fig. 7 shows the result giving the RMSE between radiosonde pairs versus the distance between these radiosondes as a two-dimensional histogram with 1 mm and 200 km bin sizes. There were restrictions in the analysis as no radiosondes with a distance in between below 200 km are available. Nevertheless, a nugget effect between 4 and 7 mm was identified, which indicates the remaining RMSE even if all ground measurements were taken at a single location. Therefore, we assume that a significant part of the scatter observed was attributed to the use of two data sets with nearly comparable accuracy. Nonetheless, the comparison against radiosondes is meaningful, as radiosondes are accepted as worldwide reference

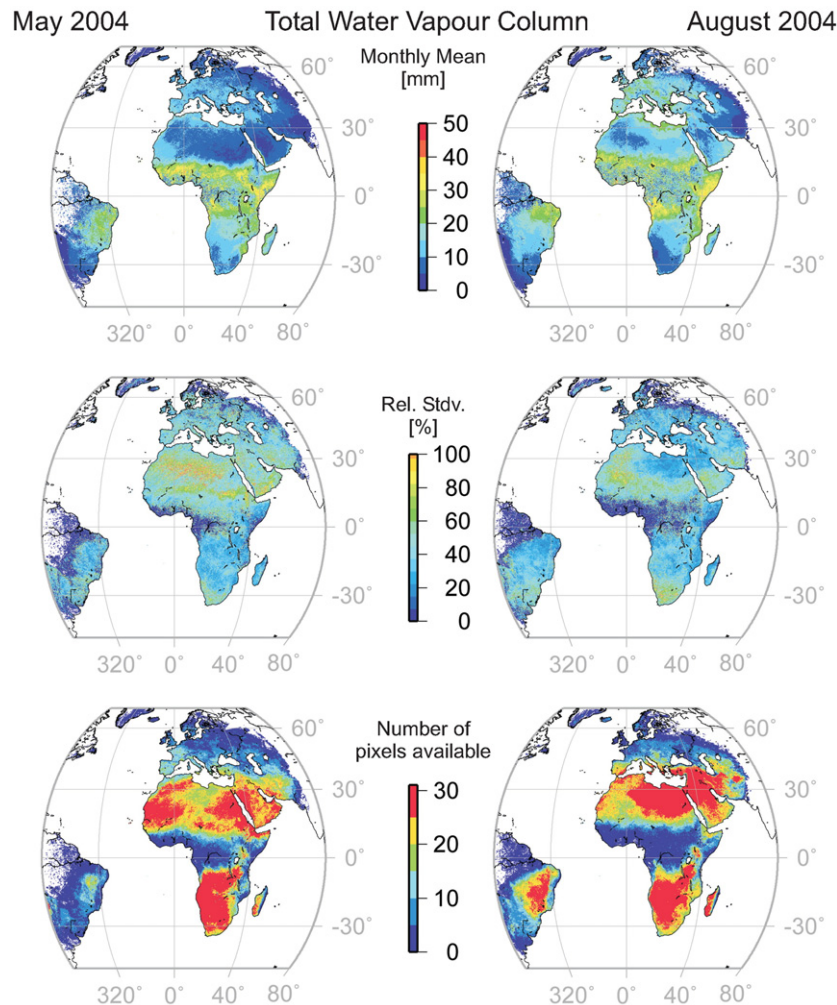


Fig. 4. MSG-SEVIRI based TWC monthly mean maps for May and August 2004 (top) together with the $1 - \sigma$ variability (middle) and the number of pixels available (bottom). White areas indicate missing values due to cloud cover, MSG field of view or presence of sea surface.

standard for temperature, humidity and total water vapor column measurements. Besides, assuming that the atmospheric situation remains the same in the time span between the two morning measurements also contributed to the miss-time scatter.

A second validation was performed against GPS measurements, as these measurements were found to be very accurate with differences in the order of 1–2 mm in TWC against ground radiometer measurements (e.g., Emardson et al., 1998). They are also available every 2 h in Europe and allow a comparison of MSG-based TWC values with a daily mean value.

The best agreement between MSG-based TWC and GPS-based TWC was found for the 9 and 11 UTC GPS measurements. The comparison with the 11 UTC GPS measurements reveals a bias of –3.0 mm and an RMSE of 6.0 mm. Fig. 8 shows a two-dimensional histogram for the 11 UTC comparison based on 287 coincidences. Differences below 5 mm are found in 90% and below 10 mm in 97% of the cases.

As the algorithm uses MSG measurements from the early and the late morning, it is not surprising to find the best agreement in the late morning. Nevertheless, for atmospheric correction and surface irradiance purposes it is necessary to understand the usefulness of this algorithm in estimating the daily mean. Therefore, the daily mean TWC value based on all clear sky GPS measurements was compared with the MSG-based TWC. Cloud clearing was performed using the MSG-based cloud detection described in Section 3.3. This study shows a bias of –2.54 mm and a slightly increased RMSE of 6.6 mm, which is still inside the accuracy limits needed for this application.

It should be noted that all GPS comparisons reported in the previous sections were restricted to GPS measurements below 45° N as the BADC radiosonde data set is available only for this region in the analysed time period. On the other hand, the GPS network provides measurements also up to higher latitudes. Above 50° N a remarkably large number of MSG-based retrievals with large differences up to 20 mm was found. These cases show

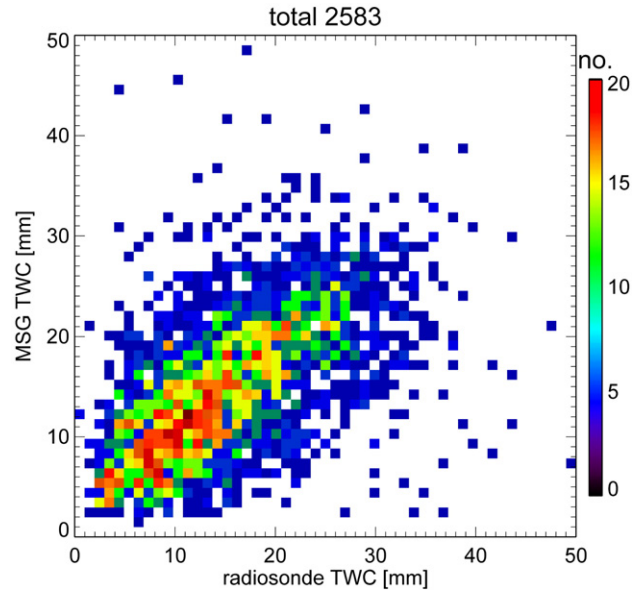


Fig. 6. Two-dimensional histogram for MSG-SEVIRI-based TWC versus European and African radiosondes obtained from the British Atmospheric Data Center (BADC) for the period March to August 2004. 94% of the differences can be found within a 10 mm range and 82% of the differences are within a 5 mm range. While there is a remarkable scatter with a low correlation coefficient of 0.59, there is also a remarkable maximum of coincidences found around the identity line.

typically very low MSG values below 5 mm, while the GPS measurement is above 20 mm. It is assumed that the cloud detection scheme fails more frequently during the morning in northern regions with both large satellite and sun zenith angles. Therefore, in these cases the water vapor absorption signal in both split-window channels is weak and results in extremely low TWC values. It is assumed that the same effect occurs for all areas with large satellite zenith angles in the MSG field of view. A further

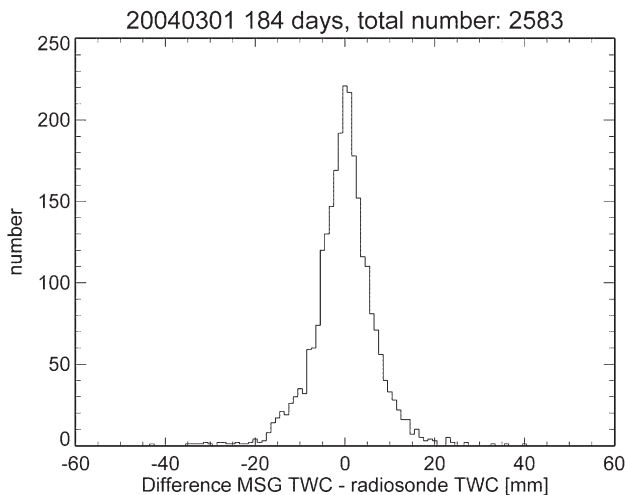


Fig. 5. Histogram of differences between MSG-SEVIRI-based and radiosonde-based total water vapor column (TWC). For the period from March to August 2004 a data set of 2583 European and African radiosondes coincidences was used. The distribution is equally distributed and peaks at the zero difference with a mean bias error of –0.2 mm and an RMSE of 6.8 mm.

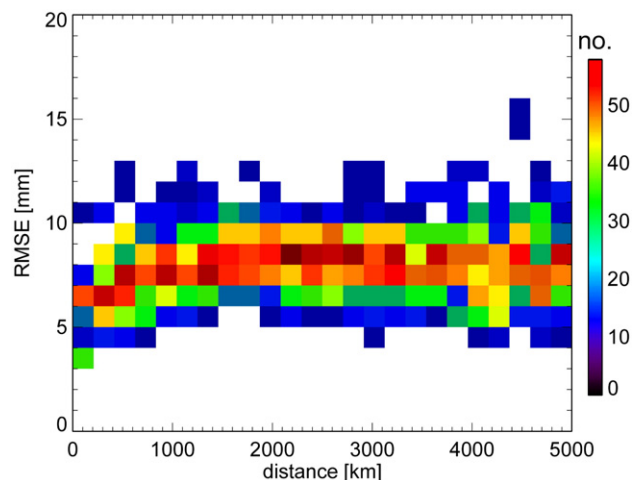


Fig. 7. Semi-variogram analysis of the European and African radiosonde data set used for validation with a bin size of 200 km and 1 mm. A nugget effect between 4 and 7 mm can be identified. It is assumed from this analysis that a significant part of the scatter observed in Fig. 6 can be attributed to the accuracy of the radiosonde data set itself.

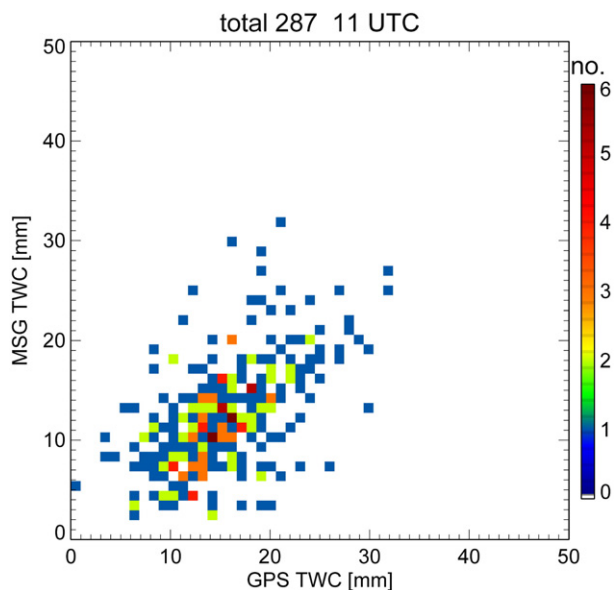


Fig. 8. Two-dimensional histogram for MSG-SEVIRI based TWC versus 11 UTC GPS measurements based on 287 coincidences for the period from March to August 2004. TWC differences below 5 mm are found in 90% and below 10 mm in 97% of the cases.

refinement of the cloud clearing procedure will probably be needed to cope with large satellite zenith angles cases.

The radiosonde and GPS comparisons with the MSG TWC values compare very well in terms of the RMSE but differ in the bias. While the comparison against radiosoundings has a neglectable mean bias error of -0.2 mm, the GPS comparison has a bias of -3 mm. It should be taken into account that the development basis for the MSG method was the TIGR3 data set which is a collection of radiosoundings representing natural variability. This might explain the better agreement in terms of the bias.

5. Conclusions

The aim of the study was to develop a retrieval scheme for total water vapor column applicable for the MSG instrument SEVIRI and suitable for operational near-real-time use on a daily basis. This paper presented an assessment of the Kleespies and McMillin (1990) approach to derive TWC over cloud-free land surfaces from thermal infrared split window channels at 10.8 and 12 μm . This method used measurements taken in two situations during the day with varying surface temperatures, assuming a constant atmospheric composition. The MSG-SEVIRI instrument with its 15 min temporal resolution allows exploitation of the daily variation in surface temperature over land, and thus validates this approach.

MSG-SEVIRI brightness temperatures were simulated for a large radiosonde test data set (TIGR3) using MODTRAN 3.7 radiative transfer simulations. The TIGR3 radiosonde data set provides globally representative temperature and humidity information. The Kleespies and McMillan approach was applied to these simulated measurements and compared with the radiosonde measurement of TWC itself. These simulations

showed a significant deviation from the linear relationship of the transmission ratio proposed by Kleespies and McMillan for small and large values of TWC. Reasons for this behavior were assumably non-neglectable absorption by other atmospheric absorbers and a saturation of water vapor absorption lines, respectively. Therefore, parameterization using a third order polynomial fit function as a function of the transmission ratio term was elaborated. Additionally, a dependence of this relationship on satellite zenith angle and air mass was found. This could not be covered by the originally proposed simple cosine correction, but was smooth enough to be parameterized with a second order polynomial fit function.

The proposed new parameterization was applied to several months of MSG-SEVIRI data (March–August 2004 in Europe and May, July and August 2004 for the full field of view of MSG covering also Africa and parts of South America). Monthly means for the full MSG field of view were presented with pixel-wise resolution for May and August 2004 together with plots of the $1-\sigma$ variability for each month. These variability maps showed the need to use daily TWC measurements instead of a monthly mean climatology in surface irradiance calculations for solar energy applications.

Comparisons with European and African radiosondes archived at the BADC data center confirm a small mean bias deviation of -0.2 mm and an RMSE of 6.8 mm. This RMSE value was very close to the accuracy range from 4 to 7 mm inherent in the radiosonde data set itself, which was assessed with a semi-variogram analysis. Therefore, we assumed that the observed scatter in satellite based TWC values versus radiosonde-based TWC values is due to comparing two data sets with nearly comparable accuracy. Further analysis revealed neither a significant seasonal dependence in relative TWC errors nor a latitudinal structure within the comparison data set. Also, no significant dependence on air temperature profile characteristics was found.

A second comparison with European GPS TWC measurements reveals the best agreement with the 11 UTC measurement with a bias of -3.0 mm and an RMSE of 6.0 mm. Two-hourly GPS measurements allow also for comparison of the cloud-free GPS-based daily mean value with the MSG-based TWC resulting in a bias of -2.6 mm and an RMSE of 6.8 mm.

The method proposed is restricted to land pixels from MSG which provide two cloud-free measurements during the night or early morning and noon hours with a minimum difference in brightness temperature of 5 K. Simulations taking the specified SEVIRI radiometric noise into account showed that a value between 5 and 10 K is required as minimum surface temperature difference. Therefore, the value of 5 K will be a subject of further optimization when MSG-SEVIRI data from several years are available. Nevertheless, asking for any minimum temperature difference between the two individual measurements during the daily temperature cycle restricts applicability in snow covered regions or wetlands. An additional restriction is due to the need for these two measurements to be cloud-free. This can clearly be seen in tropical regions or northern Europe, where the number of retrievals was significantly lower. Comparison with GPS measurements shows that large differences up to 20 mm occur in higher latitudes above 50°N in Europe. It is assumed

that these cases can be attributed to failures in the cloud clearing procedure in cases with both large sun and satellite zenith angles.

Finally, it can be stated that a retrieval method for daily TWC measurements was elaborated which is accurate enough to be used for surface irradiance calculations in atmospheric correction and solar energy applications. The restrictions to cloud-free regions are acceptable for these applications, as in case of clouds the cloud itself is the dominating element influencing surface irradiance. Also, the restriction to land surfaces is acceptable as solar energy power plants are currently not foreseen to be installed offshore. The method will be included in the operational MSG processing chain within the ESA ENVISOLAR project (<http://www.envisolar.com>). Once a larger data set of MSG-SEVIRI data covering several years and all seasons is available, an optimized value of the minimum surface temperature difference requirement will be further assessed. Additionally, further validation against other satellite-based and ground based TWC measurements, e.g., from the Global Positioning System, is foreseen.

Acknowledgements

The authors wish to thank Dr. G. Anderson (Air Force Research Laboratory, USA) for providing the MODTRAN 3.7 program; Dr. N. Scott and Dr. R. Armante (Laboratoire de Météorologie Dynamique, LMD, France) for providing the Thermodynamic Initial Guess Retrieval (TIGR3) radiosonde data set for simulations; Folke Olesen and Frank Göttsche (Institut für Meteorologie und Klimaforschung, Universität Karlsruhe) for their NOAA AVHRR land surface temperature data set for sensitivity studies; the British Atmospheric Data Center (BADC) for access to a radiosonde data set; the Geoforschungszentrum Potsdam for access to the GPS data set; and the European Union (Fifth Framework Program project HELIOSAT-3, ENK5-CT-2000-00332) for the financial support.

References

- Abreu, L.W., Anderson G.P. (Hrsg.) (1996). The MODTRAN 2/3 Report and LOWTRAN 7 Model. Philips Laboratory Hanscom, MA, USA.
- Berk, A., Anderson, G. P., Acharya, P. K., Chetwynd, J. H., Bernstein, L. S., Shettle, E. P., et al. (1999). *MODTRAN 4 user's manual*. Hanscom, MA, USA: Air Force Research Laboratory.
- Bevis, M., Businger, S., Chiswell, S., Herring, T. A., Anthes, R. A., Rocken, C., et al. (1994). GPS meteorology: mapping zenith wet delays onto precipitable water. *Journal of Applied Meteorology*, 33, 379–386.
- Chédin, A., Scott, N. A., Wahiche, C., & Moulinier, P. (1985). The improved initialization method: a high resolution physical method for temperature retrievals from satellite of the TIROS-N series. *Journal of Applied Meteorology*, 24, 128–143.
- Chesters, D., Robinson, W. D., & Uccellini, L. W. (1987). Optimized retrievals of precipitable water from the VAS 'Split-Window'. *Journal of Climate and Applied Meteorology*, 26, 1059–1066.
- Chesters, D., Uccellini, L. W., & Robinson, W. D. (1983). Low-level water vapor fields from VISSR Atmospheric Sounder (VAS) 'Split-Window' channels. *Journal of Climate and Applied Meteorology*, 22, 725–743.
- Emardson, G., Elgered, G., & Johannson, J. (1998). Three months of continuous monitoring of atmospheric water vapour with a network of GPS receivers. *Journal of Geophysical Research*, 103, 1807–1820.
- EUMETSAT Satellite Application Facility to Nowcasting and Very Short Range Forecasting (2005). Software User Manual for the PGE06 of the SAFNWC / MSG: Scientific Part, Code SAF/NWC/IOP/INM/SCI/SUM/06, Issue 1.2, Rev. 2.
- Gesell, G. (1989). An algorithm for snow and ice detection using AVHRR data: an extension to the APOLLO software package. *International Journal of Remote Sensing*, 10(4 and 5), 897–905.
- Guillory, A. R., & Jedlovec, G. J. (1993). A technique for deriving column-integrated water content using VAS Split-Window data. *Journal of Applied Meteorology*, 32, 1226–1241.
- Holzer-Popp, T., Bittner, M., Borg, E., Dech, S., Erbertseder, T., Fichtelmann, B., et al. (2001). Das automatische Atmosphärenkorrekturverfahren Durchblick*. Published in: Blaschke, T. (Hrsg). Fernerkundung und GIS: Neue Sensoren — innovative Methoden. H. Wichmann Verlag, Heidelberg, ISBN 3-87907-369-4.
- Jedlovec, G.J. (1987). Determination of atmospheric moisture structure from high-resolution MAMS radiance data. PhD dissertation, University of Wisconsin–Madison, 187 pp. [Available from University Microfilms International, 300 North Zeeb Road, Ann Arbor, MI 48106–1346].
- Kleespies, J. T., & McMillin, L. M. (1984). Physical retrieval of precipitable water using the Split Window technique. Conference on Satellite Meteorology. *Remote Sensing and Applications (AMS)*, 55–57.
- Kleespies, J. T., & McMillin, L. M. (1990). Retrieval of precipitable water from observations in the Split Window over varying surface temperatures. *Journal of Applied Meteorology*, 29, 851–862.
- Kriebel, K. T., Gesell, G., Kästner, M., & Mannstein, H. (2003). The cloud analysis tool APOLLO: improvements and validation. *International Journal of Remote Sensing*, 24, 2389–2408.
- Kriebel, K. T., Saunders, R. W., & Gesell, G. (1989). Optical properties of clouds derived from fully cloudy AVHRR pixels. *Beiträge zur Physik der Atmosphäre*, 62(3), 165–171.
- Lindau R. (2004). Gridding/ Merging Techniques for the Humidity Composite Product of the CM-SAF, Visiting Scientist Report, German Weather Service (DWD), <http://www.cmsaf.dwd.de>
- Meßinger, N. (1993). Höhenabhängige Atmosphärenkorrektur von AVHRR-Messungen zur Bestimmung von Landoberflächentemperaturen, Diploma Thesis, Institut für Meteorologie und Klimaforschung, Universität Karlsruhe (TH), Deutschland.
- Müller R. (2001) Energy-specific solar radiation data from Meteosat Second Generation (MSG) — The Heliosat-3 project, deliverable D2 "Compilation of data requirements", EU, contract NNE5-2000-00413, <http://www.heliosat3.de>
- Saunders, R. W., & Kriebel, K. T. (1988). An improved method for detecting clear sky and cloudy radiances from AVHRR data. *International Journal of Remote Sensing*, 9, 123–150.
- Schmetz, J., Pili, P., Tjemkes, S., Just, D., Kerkmann, J., Rota, S., et al. (2002). Radiometric performance of SEVIRI. *Bulletin of the American Meteorological Society*, ES50–ES51.
- Schmugge, T., French, A., Ritchie, J., Rango, A., & Pelgrum, H. (2002). Temperature and emissivity separation from multispectral thermal infrared observations. *Remote Sensing of Environment*, 79, 189–198.
- Suggs, R. J., Jedlovec, G. J., & Guillory, A. R. (1998). Retrieval of geophysical parameters from GOES: evaluation of a Split-Window technique. *Journal of Applied Meteorology*, 37, 1205–1227.